Food Control 148 (2023) 109653

Contents lists available at ScienceDirect

Food Control

journal homepage: www.elsevier.com/locate/foodcont

Non-invasive monitoring of potato drying by means of air-coupled ultrasound

Virginia Sanchez-Jimenez [a], Gentil A. Collazos-Escobar [a], Alberto González-Mohino [b], Tomas E. Gomez Alvarez-Arenas [c], Jose Benedito [a], Jose V. Garcia-Perez [a,*]

[a] Department of Food Technology, Universitat Politècnica de València, Cami de Vera, s/n, E46022, Valencia, Spain
[b] Department of Food Technology, Research Institute of Meat and Meat Products, Faculty of Veterinary, Universidad de Extremadura, Avenida de la Universidad s/n, E10003, Cáceres, Spain
[c] Institute for Physical and Information Technologies, CSIC, Serrano 144, E28006, Madrid, Spain

ARTICLE INFO

Keywords:
Drying
Potato slices
Texture
Air-coupled ultrasound
Non-invasive
Predictive model

ABSTRACT

Air-coupled ultrasound could be considered a suitable on-line technique for the non-invasive industrial testing of potato products manufactured in slices such as dried, fried or baked potato chips. Thus, the aim of the present study is to test the feasibility of air-coupled ultrasound to monitor the modifications in the physicochemical parameters of potato slices caused by drying. For that purpose, the potato slices (6 mm) were air dried (60 °C) for different drying times (15, 90, 180, 300 and 420 min). Air-coupled ultrasonic measurements were taken using through-transmission mode (250 kHz) and different compositional and textural parameters were measured. During drying, the ultrasonic velocity and the impedance increased significantly ($p < 0.05$) from 509 m/s (raw) to 673 m/s (dried for 420 min) and from 0.544 MRayl (raw) to 0.844 MRayl (dried for 420 min), respectively. Furthermore, a reduction was observed in the material attenuation, which was computed by the increase in the variation of the transmission coefficient with frequency (ΔTC_f). A principal component regression (PCR) model was successfully trained and validated and it demonstrated the potential capacity of the computed ultrasonic parameters to predict the apparent elastic modulus (E) ($R^2 = 0.96$) and the Total Relaxation Capacity (TRC) ($R^2 = 0.99$) during the drying of potato slices. The ultrasonic analysis and experimental set-up proposed in this study may be easily implemented and tested with other products, such as dried, fried or extruded snacks based on fruits or vegetables, for industrial quality control purposes.

1. Introduction

Potato snacks manufactured by frying, drying or baking are popular products whose industrial transformation involves great moisture loss, which is essential both for ensuring sample stability and for achieving specific quality attributes. Different physicochemical parameters are modified during potato processing, such as density, porosity, water activity and textural properties (Aprajeeta, Gopirajah, & Anandharamakrishnan, 2015; Dehghannya, Bozorghi, & Heshmati, 2018; Halil, Tamer, Suna, & Özkan Karabacak, 2020). In that sense, the textural properties of dehydrated potato snacks are one of the main quality parameters. However, instrumental techniques with which to assess textural attributes are destructive and highly time-consuming and can only be applied to very small batches of the total production. Therefore, there is a rising demand in the food industry for non-invasive and real-time measurement techniques to monitor quality industrial attributes (Jambrak, Nutrizio, Djekić, Pleslić, & Chemat, 2021; Tian & Xu, 2022). In addition, the digital challenge of Industry 4.0 or Smart Manufacturing considers the research into novel and efficient sensors to be of paramount importance.

Electromagnetic-based technologies are what are most frequently used for the non-invasive inspection of food materials. Thus, nuclear magnetic resonance (NMR), Near infrared (NIR), Hyperspectral imaging (HI), X-Ray computed tomography (CT), and Raman spectroscopy techniques are just some examples of these technologies used for monitoring food quality properties (Soltani Firouz, Farahmandi, & Hosseinpour, 2019; Tian & Xu, 2022). However, these techniques present some drawbacks which hinder their full implementation at industrial level, such as the great investment and high maintenance cost (NMR, CT, Raman), the fact that the inspection is limited to the surface

* Corresponding author.
E-mail address: jogarpe4@tal.upv.es (J.V. Garcia-Perez).

https://doi.org/10.1016/j.foodcont.2023.109653
Received 28 July 2022; Received in revised form 2 December 2022; Accepted 20 January 2023
Available online 25 January 2023

or the most superficial layers (NIR), the complex calibration requirement (HIS, NIRS) and the low degree of sensitivity for low moisture samples, such as dried snacks (NMR) (Feng, Zhang, & Adhikari, 2014; Tian & Xu, 2022; Xiaobo, Xiaowei, & Povey, 2016). In this context, ultrasonic technologies, widespread in other sectors, represent an affordable alternative to electromagnetism for the industrial characterisation of foods (Elfawakhry, Hussein, & Becker, 2013; Koksel, Scanlon, & Page, 2016).

The characterisation of materials by using ultrasound is based on the analysis of the ultrasound wave propagation through the inspected material, which affects both the wave velocity and attenuation and their frequency response. Ultrasound is a type of mechanical wave with a frequency higher than 20 kHz and is very sensitive to the mechanical properties of the medium in which it is propagated. Ultrasound application has great potential as a means of meeting specific industrial needs, such as affordable cost, a great penetration capacity through food materials, a fast measurement and data analysis and an easy and safe implementation (Fariñas, Contreras, Sanchez-Jimenez, Benedito, & Garcia-Perez, 2021; Kerhervé et al., 2019; Mohd Khairi, Ibrahim, Md Yunus, & Faramarzi, 2016). Conventional ultrasound techniques have been used to characterise vegetables and fruits by assessing different ultrasonic parameters, such as attenuation for avocado firmness (Flitsanov, Mizrach, Liberzon, Akerman, & Zauberman, 2000) and ultrasonic velocity for the dried orange peel firmness (Camarena, Martínez-Mora, & Ardid, 2007). However, conventional ultrasound measurements are characterised by the requirement of contact between the sample and the sensor or transducer. The purpose behind this contact is to prevent the presence of air and maximise the energy introduced into the sample and is achieved by using coupling materials (water, oil, or glycerine) or by tightly pressing the transducer on the product surface. Thus, ultrasonic contact techniques could limit any food inspection, considering the high risk of cross-contamination, or the possible surface alteration caused by both the transducer attachment and pressing or the use of coupling materials. In addition, the non-regular surface and fragility of dehydrated vegetables hinder the necessary contact with the ultrasonic transducers in conventional contact techniques, this drawback being more noticeable in the case of industrial implementation and real-time inspection. In recent years, great advances have been made in the development of efficient and reliable air-coupled piezoelectric transducers, which allow a contactless ultrasonic inspection (Garcia-Perez, de Prados, Martinez, Gomez Alvarez-Arenas, & Benedito, 2019; Ginel & Alvarez-Arenas, 2019; Kelly et al., 2001, 2001l, pp. 965–968varez-Arenas, 2004). Recent studies have illustrated the capability of this technology to characterise the mechanical properties of noodle dough using airborne ultrasound at industrial level (200 kHz) (Kerhervé et al., 2019) or meat products (Corona et al., 2013; Fariñas, Contreras, et al., 2021). However, the high attenuation of fruits and vegetables has constrained the use of airborne ultrasonic inspection in this kind of products (Fariñas, Sanchez-Torres, et al., 2021). Thereby, there is a lack of literature about the application of air-coupled ultrasound technique not only on fresh vegetables but also on the processed products. The noticeable compositional and textural modifications to potato caused by drying could potentially be assessed by using air-coupled ultrasound (Mizrach, 2008; Ozuna, Álvarez-Arenas, Riera, Cárcel, & Garcia-Perez, 2014). This positions air-coupled ultrasound as a technique of great potential for the characterisation of potato snacks but, at the same time, its application represents a challenge, due to the high degree of attenuation of this kind of product (Soltani Firouz et al., 2019). Therefore, the aim of this study was to monitor the drying of potato slices using air-coupled ultrasound as a rapid, non-destructive, and non-invasive technique in order to characterise the physicochemical modifications undergone by the product. Specifically, the changes in moisture, water activity, density, thickness and textural properties were analysed.

2. Materials and methods

2.1. Raw sample

Raw red potatoes (*Solanum tuberosum* var. Mozart) were purchased from a local market (Valencia, Spain) and stored in a dark and cold (4.0 ± 1.0 °C) room at a relative humidity of over 70% for less than 4 days (Ducreux et al., 2020). Before drying, the potatoes were washed and sliced (6 mm thick) (CL50, Robot Coupé, France). Thickness was selected from preliminary tests in which slices of 2, 4 and 6 mm were tested as usual figures in potato snack industry in the range from thin to thick samples. As the ultrasonic measurement was feasible for all the slices, 6 mm slices were chosen as the most adverse condition for ultrasonic propagation in potato due to its high attenuating nature. Afterwards, the ultrasonic, instrumental texture and compositional analyses were carried out using raw and dried potato slices at different times.

2.2. Drying experiment

The potato slices were dried for different times (15, 90, 180, 300, and 420 min) in a convective oven at 60 °C (FD 260, Binder GmbH, Germany), 0.8 m/s and 8.7% of relative humidity. The samples were periodically weighed in order to monitor the drying process. For each drying time, 10 slices were used and the process was carried out in triplicate (total of 30 slices per drying time).

2.3. Texture analysis

The potato slices were cut into square samples (10 × 10 mm) to guarantee an adequate contact between their surface and the holding plate. Approximately 10 square samples were obtained from each slice, avoiding the edges (2 mm). The viscoelastic properties of the potato slices were analysed by means of a stress-relaxation test using a texture analyser (TA. XT2i, Stable Micro Systems, Surrey, UK) placed in a temperature-controlled room (22.0 ± 1.0 °C). Thus, square potato samples were compressed using a 6 mm diameter cylindrical probe (SMS P/6, Aname, Madrid, Spain) at 1.5 mm/s test speed up to a strain of 20% and the position was held for 8 s. The test was carried out in the centre of each one of the 10 square samples, using 7 slices for each of the three replicates of each drying time (n = 210 per drying time). The experimental data were recorded and processed using Exponent Lite 6.1.4.0 software (Stable Micro System, Surrey, UK).

The textural parameters computed from the stress-relaxation curve were the hardness, the Total Relaxation Capacity (TRC) and the stiffness. The hardness was computed as the Maximum Force (F_{max}) of compression. The stiffness was assessed by the apparent elastic modulus (Young's modulus) (E) calculated from the slope of the initial linear pattern of the force-deformation curve. The TRC, meanwhile, was calculated following Eq. (1), which reflects the ratio between the force decay during relaxation (F_{max} minus the force measured at 8 s, F_{8s}) and F_{max} and provides insight into the plastic behaviour of the material (Bourne, 1982; Sinha & Bhargav, 2020b). The relaxation time (8 s) applied was selected according to Bourne (2002), who defined this parameter as the time required for the force to decay to 36.8% of its initial value.

$$TRC = \frac{F_{max} - F_{8s}}{F_{max}} \quad \text{Eq. 1}$$

2.4. Air-coupled ultrasound

The air-coupled ultrasonic experimental set-up is shown in Fig. 1 and is characterised by a pair of piezoelectric transducers specifically designed for providing an adequate impedance matching with the air (Ginel & Alvarez-Arenas, 2019; Kelly et al., 2001, 2001l, pp.

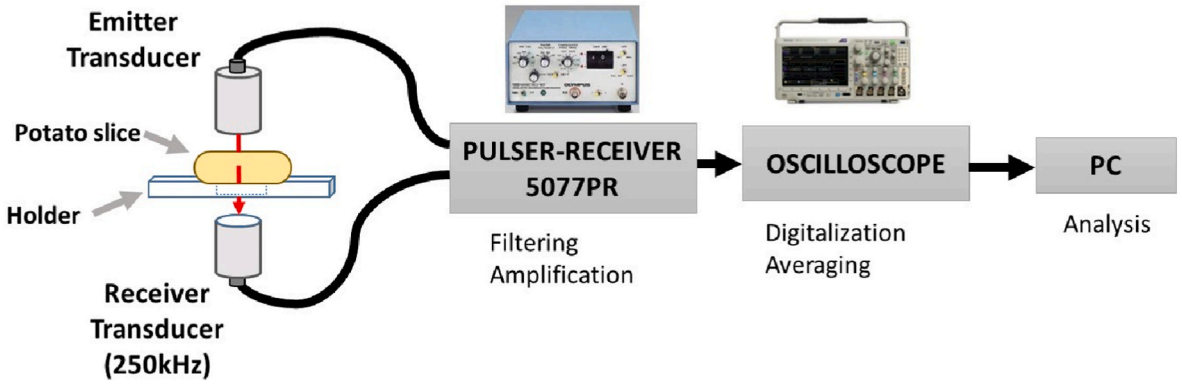

Fig. 1. Air-coupled ultrasound set-up using through-transmission mode (250 kHz).

965–968varez-Arenas, 2004). The measurements were taken in through-transmission mode, where the transmitter and receiver transducers were perfectly aligned with each other and 10 cm apart. The ultrasonic transducers presented a central frequency of 250 kHz, a bandwidth from 150 to 300 kHz, a peak sensitivity of −25 dB, an electrical impedance of 100 Ω and a diameter of 20 mm (US-BioMat lab; ITEFI-CSIC, Madrid, Spain). The pulser-receiver (5077 PR, Olympus, Houston, TX, USA) emitted a semi-cycle square wave with an amplitude of 400 V, while the gain applied to the received signal was of 59 dB. In the oscilloscope, (MDO3024, Tektronix, WA, USA) the digitalisation rate was 10 MS/s and the average signals, 128 times and 10k points, were logged using data acquisition software implemented in LabVIEW® (National Instruments, Austin, TX, USA).

For the ultrasonic analysis, the potato slices were positioned over a holding plate with a hollow (25 mm). Thus, the perfectly aligned emitter and receiver were placed over the hollow and the system was calibrated taking the ultrasonic signal travelling through the air between the transducers (air-reference), which was measured just before the analysis of each potato slice. During the ultrasonic analysis, air room conditions, relative humidity and temperature were measured (Hygrometer 608-H1, Testo SE & Co. KGaA, Lenzkirch, Germany). The measurement of the potato samples was performed by moving the slice over the plate longitudinally and recording 3 ultrasound signals per slice. Afterwards, the thickness of the slice was measured using a micrometer (±0.01 mm; Mitutoyo, Kawasaki, Japan) and averaging 7 measurements per slice.

The ultrasonic signals were analysed to determine the ultrasonic wave velocity (m/s), the acoustic impedance (Z, MRayl) and the spectrum of the transmission coefficient modulus (TC, dB). In particular, the wave velocity was determined according to Eq. (2) considering the sample thickness (h) and the time-of-flight variation (ΔTOF), which computed the difference between the TOF of the sample signal and the air-reference (Fig. 2A). The time-of-flight variation was determined by the cross-correlation method (CCM) (Garcia-Perez et al., 2019). Once the velocity was obtained, the acoustic impedance (Z) can be calculated from Eq. (3).

$$v = \frac{h}{\frac{h}{v_o} - \Delta TOF} \quad \text{Eq. 2}$$

$$Z = \rho \cdot v \quad \text{Eq. 3}$$

Where v is the ultrasonic wave velocity (m/s), h is the sample thickness (m), v_o is the velocity of sound in the air (343 m/s at 22 °C and 1 bar), ΔTOF is the time-of-flight variation (μs), Z the acoustic impedance (MRayl) and ρ the material density (kg/m^3).

The spectrum of transmission coefficient modulus (TC, dB) was calculated from Eq. (4). An example of the spectrum of the transmission coefficient is illustrated in Fig. 2B, in which it may be observed how a linear pattern appears around the central frequency of the transducer

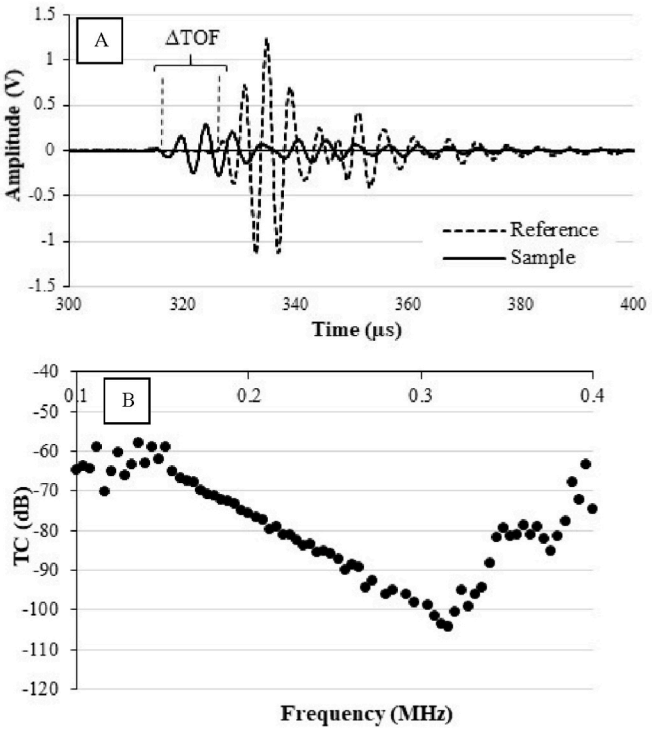

Fig. 2. A) Ultrasonic air-reference and signal transmitted through the potato slice; B) Spectrum of the transmission coefficient (TC, dB).

(from 150 to 300 kHz) (Fig. 2B). The decay in the TC may be explained by the fact that the higher the frequency, the greater the attenuation in the material. Thus, the variation in TC with the frequency (ΔTC_f, dB/MHz) was computed from the slope of the linear pattern between 150 and 300 kHz due to its relationship with the attenuation coefficient, while it is not dependent on the sample thickness.

$$TC = 20 \log\left(\frac{A}{A_0}\right) \quad \text{Eq. 4}$$

Where A and A_0 are the amplitude or modulus of the Fast Fourier Transform (FFT) of the potato sample and the air-reference signals for each frequency of the spectrum, respectively.

2.5. Moisture content and water activity

The moisture content and water activity (a_w) of the raw and dried potatoes were determined after ultrasonic and textural analyses. The moisture content was calculated by the standard gravimetric method,

drying the sample in a convection oven at 105 °C until constant weight according to AOAC method 950.46 (AOAC, 1997). The water activity analysis was determined by a dew-point hygrometer at 25 °C (Sprint th 500, NOVASINA, Switzerland). Both analyses were carried out in triplicate for each drying time.

2.6. Bulk density

The bulk density (ρ) was determined by the liquid displacement method using a pycnometer (VidraFoc, Barcelona, Spain) and toluene (Golmohammadi & Afkari-Sayyah, 2013; S. S. Nielsen, 2010). The bulk density (kg/m^3) was calculated as the ratio between the mass of the potato sample and the displaced volume of toluene, which is related with the real volume of the sample (without considering the air gaps). The experimental analysis was carried out in triplicate for each drying time.

2.7. Statistical analysis

The ultrasound (velocity, acoustic impedance, variation in the transmission coefficient with frequency and variation in time-of-flight) and physicochemical (E modulus, Total Relaxation Capacity, density and moisture content) parameters were analysed using a one-way analysis of variance (ANOVA) in order to determine whether the mean values were significantly affected by the drying time. The comparison of means was performed using Fisher's Least Significant Difference (LSD) test with a 95% confidence interval. The statistical analysis was carried out using Statgraphics Centurion XVII (Statgraphics Technologies Inc., VA, USA).

A multivariate analysis was carried out performing principal component regression (PCR) to obtain a predictive and descriptive model of the textural properties based on the ultrasonic parameters during the drying of the potato slices. To that end, a principal component analysis (PCA) was firstly applied to extract the orthogonal eigenspace and to solve the multicollinearity between the ultrasonic variables to be considered in the multiple linear regression (MLR). In this sense, all of the principal components (which account for the 100% variability of the original data set) led to the obtaining of uncorrelated scores (t) as MLR input data. For the PCA model, the drying time, the ultrasonic velocity, the acoustic impedance, the variation in the transmission coefficient with frequency and the variation in time-of-flight were considered. In order to detect and remove outlier observations from the experimental data set, multivariate control statistics, such as the residual sum of squares (RSS), and Hotelling T^2 (T^2), were used. Secondly, the MLR procedure was performed, considering t latent variables as regressors and E and TRC as responses. Finally, the training and validation of the PCR models were performed 1000 times using 75% of experimental data for model training and the remaining 25% for validation purposes. To optimise the training process, the forward-backward-stepwise variable selection was employed to screen the significant ($p < 0.05$) parameters of the regression model. In addition, the studentised residual (e_j), the leverage (V_j) and the Cook statistic (D_j) were used to find and remove defective outliers from the PCR analysis.

The goodness of fit of the regression models was assessed using the coefficient of determination (R^2) and the mean relative error (MRE). For the one-way ANOVA and PCR, the Shapiro-Wilk test and q-q plot were assessed to analyse the normality of the residuals. The Ljung-Box test was performed to verify the model residual independence and the Bartlett test was performed to test variance homoscedasticity of the model's residuals. Principal component analysis and regression procedures were carried out by employing statistical software R Core team (2021) using the R Stats Package and prcomp and lm functions, respectively. Finally, all coefficient estimations and statistical assumptions were tested with a 95% confidence level.

3. Results and discussion

3.1. Physicochemical modifications during potato drying

3.1.1. Moisture content and water activity

Raw red potato presented an average initial moisture content of 3.80 ± 0.10 kg water/kg dry matter and a_w of 0.977 ± 0.001. The hot air drying (HAD) kinetics at 60 °C of the potato slices (6 mm) are shown in Fig. 3 in which a gradual decrease in the moisture content can be observed following a typical diffusion-convection pattern. The final moisture content (420 min) was 0.11 ± 0.03 kg water/kg dry matter (Table 1), which may be considered very close to the equilibrium moisture content (Fig. 3). While the a_w was reduced from 0.977 ± 0.001 to 0.488 ± 0.001 (Table 1), ensuring microbial stability (Feng et al., 2014). Similar patterns of potato drying have been obtained by different authors (Aprajeeta et al., 2015; Hassini, Azzouz, Peczalski, & Belghith, 2007). In addition, drying involves a noticeable shrinkage (Table 1 and Fig. 3), achieving a maximum thickness reduction of 64% (Fig. 3) similar to previous published results (Jabeen, Aijaz, & Gul, 2015; Kingcam, Devahastin, & Chiewchan, 2008).

3.1.2. Bulk density

As shown in Table 1, during the drying of potato slices, the density increased gradually from 1070 ± 14 kg/m^3 in raw samples to 1275 ± 13 and 1253 ± 46 kg/m^3 after 300 and 420 min, respectively. This result coincides with the data reported by Aprajeeta et al. (2015), who reported a bulk density change from 1055 to 1273 kg/m^3 after drying at 62 °C (420 min). As a cellular solid, the joint shrinkage and water loss of the cells results in the increase in the sample density due to the higher density of the cell tissue than the water. This can be of importance when analysing the mechanical response, as this feature points to the fact that there is significant cellular deformation: initial cell shrinkage and then cellular buckling, collapse and, eventually, densification, which explained the gradual increase in density. The final density reduction between 300 and 400 min can be linked to a water loss without the corresponding tissue shrinkage due to it have lost its capability to further shrink and the water loss takes place generating some air-filled porosity. In addition, it is also of interest to point out the fact the sharp increase in the density that takes place close to 180 min. This corresponds to a moisture 0.89 (kg water/kg dry matter) and shrinkage of 50%, respectively and is linked to the transition between a deformation based on cell volume reduction and a deformation based on cell collapse for potato slices. If it is assumed that the density of the cell wall (ρ_s) is about 1400 kg/m^3, and the density of the water (ρ_w) in the cells is 1000 kg m/^{3}, then the bulk density of the tissue can be calculated as a

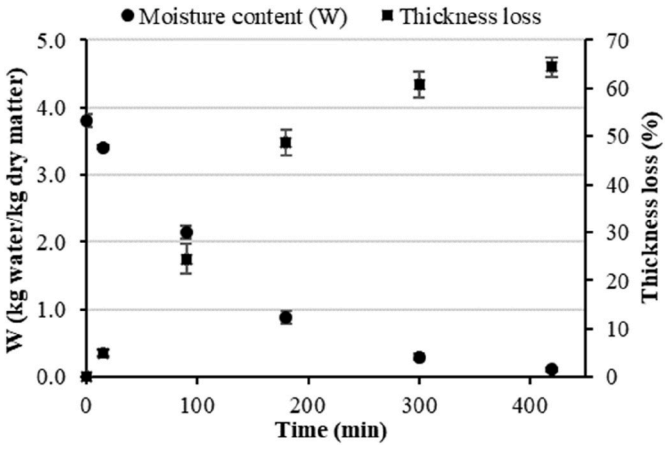

Fig. 3. Evolution of moisture content (W) and loss of thickness during the hot air drying at 60 °C of potato slices for different times (0, 15, 90, 180, 300, and 420 min). Error bars show standard error (SE).

Table 1
Physicochemical and ultrasonic parameters of potato slices dried for different times.

	Drying time (min)					
	0	15	90	180	300	420
W (kg water/kg dry matter)	3.80 ± 0.10	3.41 ± 0.03	2.14 ± 0.09	0.89 ± 0.09	0.29 ± 0.05	0.11 ± 0.03
a_w	0.977 ± 0.001	0.975 ± 0.001	0.966 ± 0.001	0.957 ± 0.001	0.725 ± 0.008	0.488 ± 0.001
h (mm)	5.94 ± 0.21	5.41 ± 0.20	4.41 ± 0.25	2.91 ± 0.20	2.21 ± 0.15	1.99 ± 0.13
ρ (kg/m^3)	1070 ± 14	1088 ± 12	1097 ± 32	1168 ± 13	1275 ± 13	1253 ± 46
F_{max} (N)	26.2 ± 1.5	25.3 ± 1.2	16.0 ± 1.0	16.1 ± 2.5	34.9 ± 6.8	37.2 ± 7.9
E (MPa)	4.44 ± 0.26	4.28 ± 0.22	2.65 ± 0.18	2.65 ± 0.44	5.96 ± 1.19	6.34 ± 1.38
TRC	0.312 ± 0.009	0.360 ± 0.011	0.468 ± 0.022	0.527 ± 0.026	0.322 ± 0.039	0.241 ± 0.033
ΔTOF (μs)	−5.32 ± 0.58	−3.61 ± 0.70	−4.42 ± 0.80	−3.37 ± 0.44	−2.43 ± 0.28	−2.55 ± 0.31
ΔTC_f (dB/MHz)	−205 ± 21	−232 ± 24	−171 ± 22	−96 ± 13	−46 ± 9	−55 ± 14
Velocity (m/s)	509 ± 5	463 ± 6	574 ± 13	607 ± 12	585 ± 11	673 ± 18
M (GPa)	0.277	0.233	0.361	0.43	0.436	0.567
Z (MRayl)	0.544 ± 0.028	0.504 ± 0.033	0.629 ± 0.071	0.709 ± 0.073	0.746 ± 0.079	0.844 ± 0.130

Mean ± standard error.
W: moisture content; a_w: water activity; h: thickness; ρ: bulk density; F_{max}: maximum force; E: elastic modulus; TRC: Total Relaxation Capacity; ΔTOF: variation in time-of-flight; ΔTC_f: variation in the transmission coefficient with frequency; Z: ultrasonic impedance; M: ultrasonic modulus.

function of the solid volume fraction (k) as follows:

$$\rho = k\rho_s + (1-k)\rho_w \quad \text{Eq. 5}$$

Thereby, at t = 0 min, $k = 0.175$, at t = 180 min, $k = 0.42$ and after 300 min, $k = 0.69$, while the inner cell volume fraction ($\varphi = 1 - k$), is 0.825, 0.58, 0.31, respectively. As already mentioned, this large average cell volume fraction reduction is consistent with the collapse of some cells and the appearance of some residual air-filled porosity at the end of drying (from 300 to 420 min).

3.1.3. Texture

Fig. 4 shows the evolution in the Elastic modulus (E, MPa) and the Total Relaxation Capacity (TRC) during drying and its relationship with the moisture content, in which two well differentiated stages may be observed. At the initial drying stage, up to a moisture content of 0.89 kg water/kg dry matter, potato slices underwent a reduction in E and an increase in TRC. Thus, E decreased from 4.44 ± 0.26 (raw) to 2.65 ± 0.44 MPa (0.89 kg water/kg dry matter) and TRC increased from 0.312 ± 0.009 (raw) to 0.527 ± 0.026 (0.89 kg water/kg dry matter). The water loss produces a loss in the internal cell pressure (loss in turgor pressure) and a loss in cell volume, as is also indicated by density measurements. These changes certainly lead to a loss in cell wall tautness and an increase in cell wall curvature. All these modifications give rise to a more compressible cell and, hence, this explains the loss in the tissue elastic modulus. This is a well-known feature of cellular solids and may be explained by the fact that the macroscopic elastic modulus of this type of solid is determined by the bending and flexing of the cell walls (Gibson & Ashby, 1997). The loss in cell wall tautness and the increase in cell wall curvature contribute to a reduction in the cell wall flexural rigidity. Moreover, this effect also contributes to an increase in the internal mobility and the degree of freedom of the cells' spatial configuration, so that the viscoelastic response grows. This explains the fact that the viscoelasticity of the potato slices increases at the beginning of drying while their resistance to deformation decreases. Thus, drying involves not only the softening of the material, F_{max} decreased from 26.2 ± 1.51 (raw, 3.80 kg water/kg dry matter) to 16.1 ± 2.50 N (0.89 kg water/kg dry matter), but also implies more viscous behaviour due to a modification of the molecular mobility leading to a more amorphous structure (Li, Lin, Roos, & Miao, 2019), and also turgor loss, as explained by Krokida et al. (2000), which could be probably linked to a glass transition. However, below that moisture range, around 0.89 kg water/kg dry matter, which could be considered critical, the potato behaved in the opposite way and the increase in E and the reduction in TRC were noticeable (Table 1, Fig. 4). Previous studies have also illustrated the observed phenomenon, reporting critical moisture contents ranging from 1.1 to 1.8 kg water/kg dry matter (Krokida, Karathanos, & Maroulis, 2000; Sinha & Bhargav, 2020a). Critical moisture content will be affected not only by the raw material but also by the drying method used, as well as other key relevant properties, such as glass transition (Nguyen, Mondor, & Ratti, 2018). Thus, below the critical moisture content 0.89 kg water/kg dry matter, the progressive cell volume reduction (with water loss) eventually leads to a point at which the tissue is subjected to a densification process through cell buckling and collapse. This involves a change in the trend of the elastic modulus due to once the cells start to collapse, the cell wall loses its capacity to bend; therefore, the macroscopic tissue elastic modulus is no longer determined by the cell wall flexural rigidity but by the cell wall rigidity. In addition, cell wall rigidity is much greater than cell wall flexural rigidity, particularly taking into account the fact that the cell wall is very thin (Gibson & Ashby, 1997). Moreover, this hypothesis about the role of cell collapse in the observed increase in E that occurs in line with the loss of water (Fig. 4) is also supported by the density measurements (Table 1).

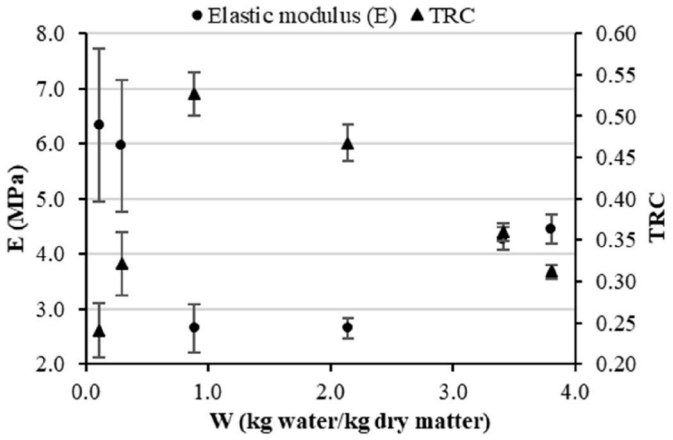

Fig. 4. Influence of the moisture content (W) on the elastic modulus (E) and Total Relaxation Capacity (TRC, dimensionless) of potato slices dried at 60 °C. Error bars show standard error (SE).

Another noticeable phenomenon that also contributes to the increase in the elastic modulus when the loss of water goes beyond a certain point is the reduction in the water potential, which leads to the decrease in the turgor potential and the reduction in the osmotic potential. However, the water in the cell wall must be in equilibrium with the water in the cells, which gives rise to a continuous reduction in the water content in the cell wall as well. Eventually, this dehydration of the cell wall gives rise to a change in the elastic and viscoelastic moduli of the cell wall. When the dehydration is high enough, the cell wall material undergoes a significant transformation, which involves a more rigid material whose flexural rigidity is also greater.

3.2. Modification of ultrasonic parameters during drying

The ultrasonic parameters analysed were the ultrasonic velocity, v, (m/s), the variation in the transmission coefficient with frequency (dB/MHz) and the acoustic impedance (MRayl). In addition, the ultrasonic

elastic modulus (M) can also be computed from velocity and density data (Table 1):

$$M = v^2\rho \quad \text{Eq. 6}$$

The big difference between M and E moduli can be explained by the different time scales used to obtain these two parameters. While for the ultrasonic measurement the deformation rate is in the range of "μs", the deformation rate for E measurements is in the "s" scale (Taiz and Zeiger, 2002; and Forterre, 2013). This is of importance because the poroelastic relaxation time in plant tissues is in the "ms" range, which means that the deformation rate in the ultrasonic measurements is so fast that the fluid in the cells has no time to flow in or out of the cell, that is, fluid significantly contributes to the measured elastic modulus. On the contrary, in E measurements, the deformation rate is slow enough so that some part of the fluid inside the cells can flow in or out the cell, so that the contribution of the fluid to the measured elastic modulus is reduced. This explain why the ultrasonic modulus, M, is much larger than the elastic modulus, E. This same result is observed when the elastic modulus of plant tissues obtained from ultrasonic and instrumental pressure chamber measurements are compared (Sancho-Knapik et al., 2011).

Fig. 5 shows the effect of the moisture content on the velocity and the ΔTC_f. The average ultrasonic velocity of the raw potato slices was 509 ± 5 m/s, which represents a slightly lower figure than that reported by Ha, Kanai, Chubachi, and Kamimura (1991) (824 m/s) when analysing the Wasesiro potato variety using contact ultrasound. These authors highlight the high degree of experimental variability of the ultrasonic velocity (standard deviation of 112 m/s), which can explain the observed differences particularly if different potato varieties are compared. The low ultrasonic velocity in vegetables is explained by their structure, which is generally made up of a large porous network that can be empty (high porosity vegetables) or filled with liquid water (low porosity vegetables). In this cellular structure, as commented on before, the bulk compressibility is determined by the cell wall flexural rigidity, which can produce very low values of the elastic modulus. Moreover, in the case of plant tissues, this cellular structure is filled with a fluid, so bulk tissue density increases. Considering that the longitudinal ultrasound velocity (v_L) is given by Eq. (7):

$$v_L = \sqrt{\frac{K + \frac{4}{3}\mu}{\rho}} \quad \text{Eq. 7}$$

where K is the bulk compressibility modulus, μ is the bulk rigidity modulus (sometimes $K + \frac{4}{3}\mu$ is known as the ultrasonic modulus: M, see Eq. (6) and Table 1) and ρ the apparent density (Laugier & Haiat, 2016; Mohd Khairi et al., 2016), the presence of water in plant tissues can give rise to lower velocity values compared to other cellular solids. Actually, the figures found for potato (Table 1) are similar to the values measured for other palisade parenchyma tissues.

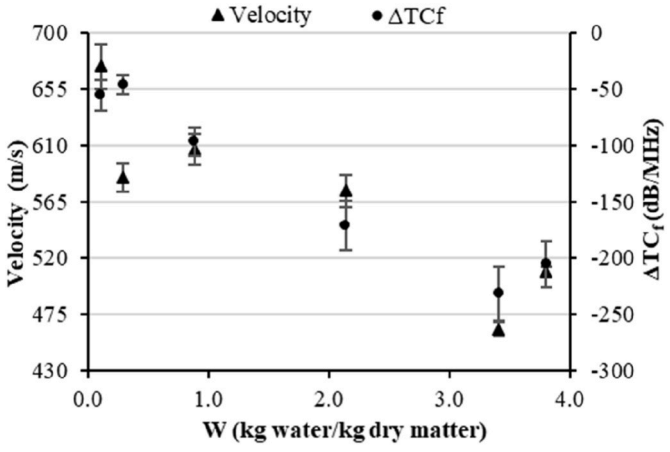

Fig. 5. Influence of the moisture content (W) on the ultrasonic velocity and the variation in the transmission coefficient in line with frequency (ΔTC_f) of potato slices dried at 60 °C. Error bars show standard error (SE).

Ultrasound velocity (Table 1) initially decreases (from 509 m/s to 463 m/s, during the first 15 min of drying). This reduction is due to the fact that the density is increasing and the elastic modulus decreasing. As observed in Figs. 3 and 4, the trend in the variation in the ultrasonic velocity in line with the water loss also changes. According to Table 1, somewhere between min. 15 and min. 90, the ultrasonic velocity starts to increase. This time range corresponds to W values between 2 and 3 kg water/kg dry matter. Considering that density increases throughout the whole drying process, this must be due to an increase in the ultrasonic elastic modulus (see Eq. (6)). According to Table 1, the ultrasonic modulus decreases from min t = 0 up to min t = 15, and then starts to increase at some point between min 15 and 90. However, Fig. 4 reveals that E only increases when W falls to under 1 (kg water/kg dry matter). The fact that the change in trend of the ultrasonic modulus takes place earlier (higher W values) when compared with the change in E can also be explained by the different natures of E and M, as the former is obtained at a deformation rate slower than the poroelastic relaxation time while the latter is obtained at much faster deformation rates. Given that the fluid compressibility contributes greatly to the measured M modulus, the fact that this trend is observed to change in earlier is not wholly unexpected.

On the one hand, the initial decrease in the ultrasonic velocity and ultrasonic modulus may also be observed in the study of other plant tissues and is well reported in the case of plant leaves, where it has been fully determined that the decrease in the ultrasonic velocity in line with the loss in relative water content, RWC (typically from RWC = 1 to RWC 0 = 0.7), can be linked to the loss in turgor and the increased cell compressibility due to the associated loss in cell wall tautness (Sancho-Knapik et al., 2011). On the other hand, the further increase in velocity that occurs in line with the loss in water can be linked to more radical changes in the tissue, as explained before. The ultrasonic velocity increased significantly ($p < 0.05$) during drying, up to 673 ± 18 m/s for a moisture content of 0.11 kg water/kg dry matter. The increase in the ultrasonic velocity during drying was also described by Camarena et al. (2007) when studying orange peel dried by natural convection at room temperature for 60 days (from 150 to 200 m/s). These authors measured the ultrasonic velocity by using through-transmission contact techniques at 50 kHz and evidenced a high degree of uncertainty in the measurement, which was mainly ascribed to the measurement of the sample thickness.

The effect of the reduction in the moisture content on the ultrasonic velocity has also been highlighted for other kinds of products. Benedito, Carcel, Gisbert, and Mulet (2001) characterised the maturation of cheese by contact ultrasound (1 MHz), recording an ultrasonic velocity increase from 1630 to 1750 m/s during the curing time (≤400 d). Meanwhile, García-Álvarez, Salazar, and Rosell (2011) observed a change, from 70 to 170 m/s (at 100 kHz), caused by a reduction in the moisture content of bread dough. The increase in velocity is linked to both the moisture loss and the modifications in the sample's elastic behaviour. On the one hand, the water loss will result in a faster ultrasound propagation, since the velocity in the solid matrix is generally higher than in water. However, this behaviour could be hindered by an increase in the air fraction occupying the pores if the shrinkage is mild. On the other hand, the considerable initial moisture content reduction should increase the ultrasonic velocity owing to the greater sample density (Table 1); however, the reduction in the elasticity (Fig. 4) leads to a slight decrease in the velocity at those drying times. Therefore, structural modifications will also impact on the mechanical properties and definitively affect the ultrasonic propagation velocity.

The high degree of attenuation of the potato prevented the measurement of the attenuation coefficient since neither reverberations nor the second pulse was detected. Fig. 5 shows the effect of the moisture

content on the change in the variation of the transmission coefficient in line with the frequency (ΔTC_f), which is a useful index for the purposes of measuring the energy absorption or attenuation, since the higher the ΔTC_f, the larger the amount of energy transmitted through the material. The behaviour of ΔTC_f was very similar to that of the ultrasonic velocity; thus, it changed from -205 ± 21 (raw, 3.80 kg water/kg dry matter) to -55 ± 14 dB/MHz (0.11 kg water/kg dry matter). Therefore, the increase in ΔTC_f followed a linear pattern as the moisture content decreased, which reflects the fact that the energy loss brought about by absorption diminishes as dehydration progresses. Kang-lyeol et al. (1991) found attenuation coefficients in raw potato from 0.1 dB/mm at 50 kHz to 10 dB/mm at 1 MHz. To our knowledge, the analysis of ultrasonic attenuation in potato at different moisture contents has not previously been addressed. The reduction in the material attenuation observed during potato drying could be ascribed to a homogenisation effect of the potato slices during drying, since the water-solid interfaces were reduced or disappeared. The compositional and structural changes in the sample during drying depend heavily not only on the product being dried but also on the dehydration method and will control the ultrasonic energy absorption. For this reason, vegetables may behave differently in terms of energy absorption, which explains the results reported by Camarena et al. (2007), who reported an increase in the attenuation coefficient (from 2.4 to 4.1 dB/mm) during drying, ascribed to the increase in the oil content.

The acoustic impedance (Z) was computed since it integrates the ultrasonic and physicochemical parameters. The Z of the raw potato was 0.544 MRayl, which is consistent with the figures reported by Ozuna et al. (2014) and McClements (1997) who found Z values for raw potato samples of 0.66 and 0.85 MRayl, respectively. Table 1 shows the evolution of Z during drying for the potato slices, in which an increase ($p < 0.05$) up to 0.844 MRayl (0.11 kg water/kg dry matter) was found in Z. The gradual increase in Z as dehydration progresses is linked to both higher ultrasonic velocity and greater density. Along those lines, some authors proposed Z as a key parameter for food quality control; for example, Salazar, Chávez, Turó, and García-Hernández (2017) reported the possible application of Z as a means of directly measuring the gas content in cake batter. These authors correlated the decrease in the Z value with the increase in the air content of the cake batter, which could be explained by the decrease in density and velocity. This explains the noticeable differences in the Z value as the potato moisture content falls. In that sense, during drying, the air and water interfaces of the potato slices are minimised, becoming a different material, in contrast with the raw potato slices. Thus, the considerable changes in the potato's physicochemical properties during drying could be related and described by ultrasonic parameters.

Fig. 6 shows the relationship between the variation in the transmission coefficient with frequency and bulk density. The relationship between both parameters followed a significant ($p < 0.05$) linear pattern ($R^2 = 0.91$); thus, the greater the density, the higher the ΔTC_f. This illustrates that drying involved a smaller acoustic energy absorption, probably linked to the increase in density (Table 1) due to the aforementioned bigger solid volume fraction. Elmehdi, Page, and Scanlon (2004) reported a linear relationship between the increase in the number of air-bubbles for a bread dough and the attenuation of the material measured by contact ultrasonic techniques (54 kHz). A similar effect was reported by Nielsen and Martens (1997) for cooked carrots, in which the density increase brought about by the removal of air as a result of boiling led to a decrease in the material attenuation (from 1.1 dB/mm to 0.5 dB/mm) measured by contact techniques at 37 kHz.

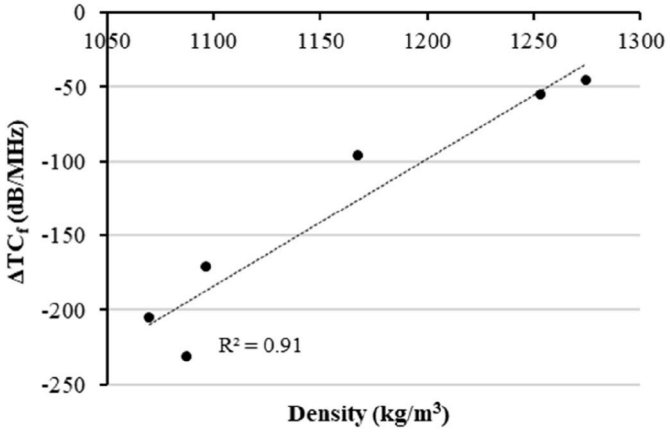

Fig. 6. Relationship between the variation in the transmission coefficient in line with frequency (ΔTC_f) and the density of potato slices dried at 60 °C.

3.3. Relationship between textural and ultrasonic parameters based on multivariate analysis

The use of digital sensors to provide robust mathematical models with which to predict the textural characteristics of this kind of product is a historical demand of the food industry. Thereby, based on a simplified form of Eq. (7), in which the ultrasonic modulus is matched to the elastic, significant linear and polynomial relationships between textural parameters, such as hardness, and the ultrasonic velocity for different foodstuffs, has been reported (Fariñas, Sanchez-Torres, et al., 2021; Mizrach, 2008; Mohd Khairi et al., 2016). In the case of vegetable drying, no previous literature has addressed the relationship between the ultrasonic velocity and the textural parameters for the whole drying process and most research has focused on the changes observed during the storage of vegetable materials, in which small variations of moisture content will occur, or in other processing stages. In this sense, Kim, Lee, Kim, and Cho (2009) related a reduction (from 1.15 MPa on day 0–0.45 MPa after 25 days) in the elastic modulus of apples during storage (at 22 °C) with a decay in the ultrasonic velocity, from 200 m/s to 80 m/s, measured by contact techniques (at 100 kHz); this coincides with the data reported in this study on the change in the elastic modulus and the ultrasonic velocity between the raw potato and the potato dehydrated for 15 min (Table 1). Therefore, the relationship between the textural and the ultrasonic parameters should be influenced by the different mechanical behaviour of the potato tissue at moisture contents above and below the critical level, as explained in detail in the previous section. This is illustrated in Fig. 7, in which second-degree polynomial functions were found when E was correlated with the ultrasonic velocity ($R^2 = 0.93$, Fig. 7A) and the acoustic impedance ($R^2 = 0.95$, Fig. 7B), which points to a different pattern dependent on the drying time. In the case of the TRC, meanwhile, the correlations with the ultrasonic velocity and the acoustic impedance were slightly poorer, with coefficients of determination of $R^2 = 0.73$ and $R^2 = 0.64$, respectively. Noticeable mathematical relationships were not found between the attenuation-related parameter (ΔTC_f) and the E and TRC textural parameters. In this context, in which not only may different variables help to explain the change in the textural parameters but the mathematical pattern may also change depending on the process time, the use of multivariate analysis methodologies is fully justified.

Principal component regression (PCR) was developed to interpret and obtain a predictive model of the evolution of the potato's textural properties during drying from ultrasonic parameters. Table 2 shows the principal components (PCs) and the loadings obtained from the PCA of the E and TRC multivariate analysis, considering the variation in time-of-flight (ΔTOF), the variation in the transmission coefficient with frequency (ΔTC_f), the ultrasonic velocity, the acoustic impedance (Z) and the drying time as the variables. The PCA aims to remove the multicollinearity between the ultrasound variables for the subsequent multiple regression analysis, separating them into orthogonal spaces (PCs). Thus, a major part of the data variability was described by PC1 (57%) and PC2 (34%), whereas PC3, PC4, and PC5 presented an explained variance of 6.7%, 2.6%, and 0.02%, respectively. But despite the poor

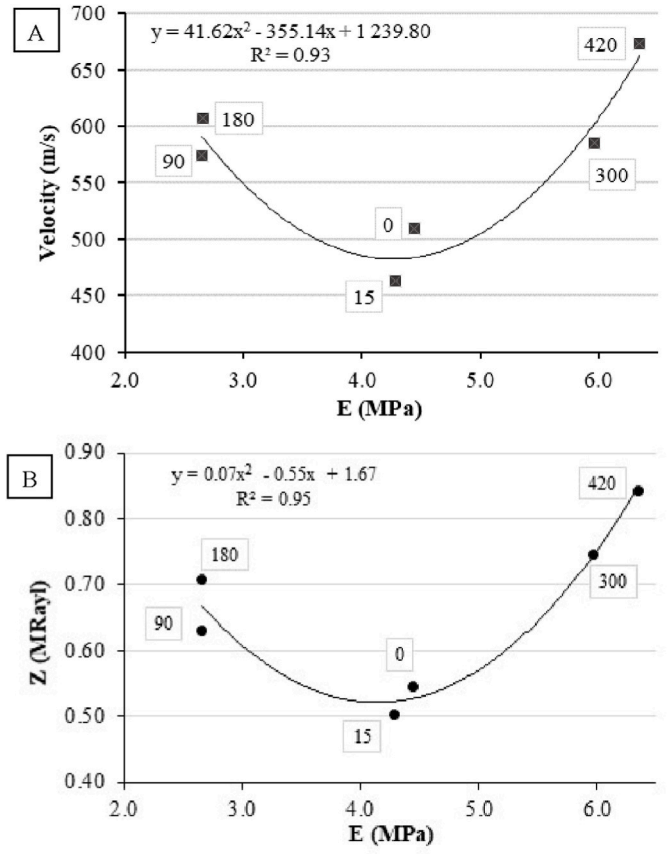

Fig. 7. Relationship between the elastic modulus (E) of potato slices dried at 60 °C and A) ultrasonic velocity and B) impedance (Z). Labels indicate the drying time, and the continuous line shows a 2nd-polynomial fit.

explained variance in some PCs, the PCA has not removed any components since they describe significant situations observed in dried samples, which must be taken into account for the subsequent MLR analysis. For instance, after relating PC2 and PC3, an inverse relationship was observed between ΔTOF and ΔTC_f, which may describe the effect observed after 15 min of drying where the ΔTOF was reduced and the attenuation of the potato increased, simultaneously (Table 1). PC5, however, reflects the fact that the relationship between the velocity and the impedance after a drying time of 300 min is inverse to what is normally observed, which may be explained by the small reduction in the density at the end of the drying. This reflects the capability of the multivariate analysis to describe the relationship between acoustic and textural parameters during the drying of potato slices.

The statistical results of model training and validation are illustrated together in Table 2. As can be observed, the results obtained reflect the high quality of the goodness-of-fit of PCR models in terms of both elastic modulus and Total Relaxation Capacity (MRE<10% and R^2>95%) indicating that both predictors can be used for practical applications due to their suitable fitting ability (Silva et al., 2021). Fig. 8A and C shows the close agreement between the experimental and predicted E (R^2 = 96.2% and MRE = 6%) and TRC values (R^2 = 99.4% and MRE = 1.59%), which evidences a successful prediction of the experimental responses. In addition, the residual validation showed random patterns ($p > 0.05$ for every test) for PCR models (Fig. 8B and D) which demonstrates the trustworthiness of the models developed to provide a highly accurate description of the textural properties of potato slices during drying.

4. Conclusions

The feasibility of the air-coupled ultrasound technique to monitor the drying process of potato slices was illustrated in this study. Computed ultrasonic parameters from the time domain and the frequency spectrum were able to explain the changes in the physicochemical parameters due to the moisture loss and structural modifications caused by drying. In addition, multivariate models were successfully developed and validated to predict the textural properties of potato slices during drying. It should be pointed out that textural modifications during drying are dependent not only on the raw potato but also on the kind of drying process and pre-treatments used, which also affect the ultrasonic parameters. Therefore, this study has demonstrated the potential of the air-coupled ultrasound techniques for the purposes of the non-invasive and real-time monitoring of potato slice drying or the characterization of the textural and compositional properties of potato snacks manufactured in slices, providing the food industry with reliable tools in the digital challenge of Industry 4.0 and Smart Processing.

Table 2
PCA loadings and statistical results of the PCR model for the elastic modulus (E) and Total Relaxation Capacity (TRC).

Variables	Loadings PCs (%explained variance and R^2)				
	PC1 (57%)*	PC2 (33.57%)*	PC3 (6.70%)*	PC4 (2.70%)*	PC5 (0.03%)*
Drying time (min)	0.654 (40%)**	−0.057 (0%)**	0.461 (21%)**	−0.593 (35%)**	−0.064 (0.1%)**
ΔTOF (μs)	0.443 (20%)**	0.680 (45%)**	0.166 (0.3%)**	0.558 (31%)**	−0.049 (0.1%)**
ΔTC_f (dB/MHz)	0.602 (35%)**	−0.340 (12%)**	−0.707 (50%)**	0.148 (0.3%)**	−0.008 (0%)**
Velocity (m/s)	0.02 (0%)**	−0.480 (23%)**	0.340 (12%)**	0.407 (17%)**	−0.699 (47%)**
Z (MRayl)	0.115 (0.2%)**	−0.433 (18%)**	0.380 (15%)**	0.387 (15%)**	0.711 (50%)**

Principal component regression (PCR)

	E		TRC	
	Regression coefficient (β)	P-value	Regression coefficient (β)	P-value
β_0	2.819	0.000	0.504	0.000
$\beta_1 t_1$	0.072	0.166	0.002	0.435
$\beta_2 t_2$	−0.213	0.002	0.083	0.000
$\beta_3 t_3$	0.064	0.558	0.112	0.000
$\beta_4 t_4$	−0.184	0.526	0.371	0.000
$\beta_5 t_5$	13.916	0.000	−1.073	0.000
$\beta_6 t_1^2$	0.765	0.000	−0.024	0.000
$\beta_7 t_1 t_2$	−0.172	0.006	0.079	0.000
$\beta_8 t_1 t_3$	1.088	0.000	–	–
$\beta_9 t_1 t_4$	−2.340	0.000	0.091	0.000
$\beta_{10} t_1 t_5$	9.544	0.000	−0.581	0.000
$\beta_{11} t_2^2$	–	–	−0.028	0.000
$\beta_{12} t_2 t_3$	–	–	0.085	0.000
$\beta_{13} t_2 t_4$	0.481	0.001	−0.093	0.000
$\beta_{14} t_3 t_4$	−1.937	0.000	0.129	0.000
$\beta_{15} t_3 t_5$	–	–	1.840	0.000
$\beta_{16} t_4 t_5$	−43.144	0.000	−0.600	0.009
MRE (%)	Training 6.00 ± 0.50 Validation 6.00 ± 1.00		Training 1.58 ± 0.35 Validation 1.59 ± 0.42	
R^2 (%)	Training 96.40 ± 0.60 Validation 96.20 ± 1.60		Training 99.50 ± 0.33 Validation 99.40 ± 0.41	

PC: principal component; t: latent variable; ΔTOF: variation in time-of-flight; ΔTC_f: variation in the transmission coefficient in line with frequency; Z: acoustic impedance; E: elastic modulus (MPa); TRC: Total Relaxation Capacity; MRE: mean relative error; R^2: coefficient of determination.
*Explained variance of each principal component.
**R^2 of the variables in each principal component.

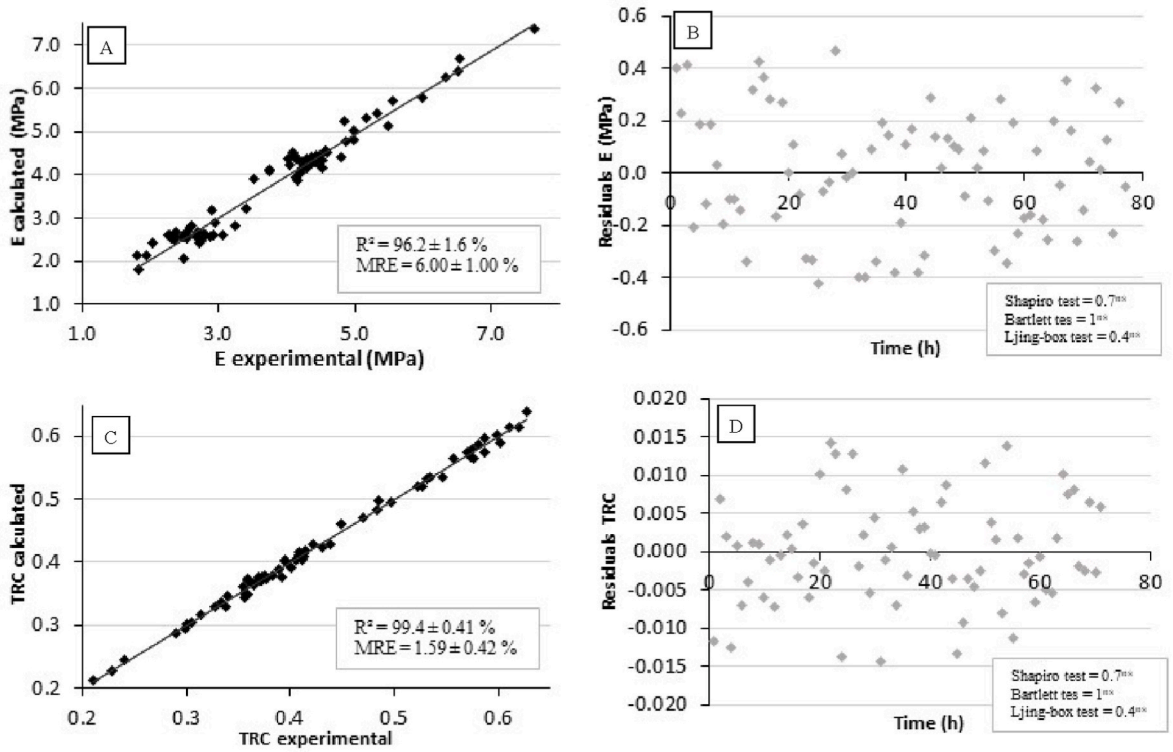

Fig. 8. Coefficient of determination (R^2) and the residuals for the principal component regression (PCR) multivariate analysis of A) the elastic modulus (E) and B) the Total Relaxation Capacity (TRC). Mean residual error (MRE) and validation test of the residual errors.

CRediT authorship contribution statement

Virginia Sanchez-Jimenez: Methodology, Formal analysis, Investigation, Writing – original draft. **Gentil A. Collazos-Escobar:** Methodology, Formal analysis, Software. **Alberto González-Mohino:** Methodology, Formal analysis, Writing – original draft. **Tomas E. Gomez Alvarez-Arenas:** Conceptualization, Methodology, Writing – review & editing. **Jose Benedito:** Formal analysis, Writing – review & editing, Supervision. **Jose V. Garcia-Perez:** Conceptualization, Methodology, Supervision, Writing – review & editing, Supervision, Project administration, Funding acquisition.

Declarations of competing interest

None.

Data availability

Data will be made available on request.

Acknowledgements

The authors acknowledge the financial support of the Universitat Politècnica de València (Project 20200421).

References

Álvarez-Arenas, T. E. G. (2004). Acoustic impedance matching of piezoelectric. *IEEE Transactions on Ultrasonics, Ferroelectrics, and Frequency Control, 51*(5), 624–633.

AOAC. (1997). Official methods 950.46. In *Official methods of analysis* (sisteenth ed.).

Aprajeeta, J., Gopirajah, R., & Anandharamakrishnan, C. (2015). Shrinkage and porosity effects on heat and mass transfer during potato drying. *Journal of Food Engineering, 144*, 119–128. https://doi.org/10.1016/j.jfoodeng.2014.08.004

Benedito, J., Carcel, J., Gisbert, M., & Mulet, A. (2001). *Quality Control of Cheese Maturation, 66*(1), 100–104.

Bourne, M. C. (1982). *Food texture and viscosity: Concept and measurement*.

Bourne, M. C. (2002). Food texture and viscosity. Concept and measurement. In *Food science and technology* (Vol. 53)Elsevier Science Imprint. https://doi.org/10.1017/CBO9781107415324.004. Issue 9.

Camarena, F., Martínez-Mora, J. A., & Ardid, M. (2007). Ultrasonic study of the complete dehydration process of orange peel. *Postharvest Biology and Technology, 43*(1), 115–120. https://doi.org/10.1016/j.postharvbio.2006.07.012

Corona, E., Garcia-Perez, J. V., Gomez Alvarez-Arenas, T. E., Watson, N., Povey, M. J. W., & Benedito, J. (2013). Advances in the ultrasound characterization of dry-cured meat products. *Journal of Food Engineering, 119*(3), 464–470. https://doi.org/10.1016/j.jfoodeng.2013.06.023

Dehghannya, J., Bozorghi, S., & Heshmati, M. K. (2018). Low temperature hot air drying of potato cubes subjected to osmotic dehydration and intermittent microwave: Drying kinetics, energy consumption and product quality indexes. *Heat and Mass Transfer/Waerme- Und Stoffuebertragung, 54*(4), 929–954. https://doi.org/10.1007/s00231-017-2202-5

Elfawakhry, H., Hussein, M. A., & Becker, T. (2013). Investigations on the evaluation of rheological properties of cereal based viscoelastic fluids using ultrasound. *Journal of Food Engineering, 116*(2), 404–412. https://doi.org/10.1016/j.jfoodeng.2012.12.021

Elmehdi, H. M., Page, J. H., & Scanlon, M. G. (2004). Ultrasonic investigation of the effect of mixing under reduced pressure on the mechanical properties of bread dough. *Cereal Chemistry, 81*(4), 504–510. https://doi.org/10.1094/CCHEM.2004.81.4.504

Fariñas, L., Contreras, M., Sanchez-Jimenez, V., Benedito, J., & Garcia-Perez, J. V. (2021). Use of air-coupled ultrasound for the non-invasive characterization of the textural properties of pork burger patties. *Journal of Food Engineering, 297*(December 2020). https://doi.org/10.1016/j.jfoodeng.2021.110481

Fariñas, L., Sanchez-Torres, E., Sanchez-Jimenez, V., Diaz, R., Benedito, J., & Garcia-Perez, J. V. (2021). Assessment of avocado textural changes during ripening by using contactless air-coupled ultrasound. *Journal of Food Engineering, 289*(July 2020). https://doi.org/10.1016/j.jfoodeng.2020.110266

Feng, L., Zhang, M., & Adhikari, B. (2014). Effect of water on the quality of dehydrated products: A review of novel characterization methods and hybrid drying technologies. *Drying Technology, 32*(15), 1872–1884. https://doi.org/10.1080/07373937.2014.963205

Flitsanov, U., Mizrach, A., Liberzon, A., Akerman, M., & Zauberman, G. (2000). Measurement of avocado softening at various temperatures using ultrasound. *Postharvest Biology and Technology, 20*(3), 279–286. https://doi.org/10.1016/S0925-5214(00)00138-1

García-Álvarez, J., Salazar, J., & Rosell, C. M. (2011). Ultrasonic study of wheat flour properties. *Ultrasonics, 51*(2), 223–228. https://doi.org/10.1016/j.ultras.2010.08.006

Garcia-Perez, J. V., de Prados, M., Martinez, G., Gomez Alvarez-Arenas, T. E., & Benedito, J. (2019). Ultrasonic online monitoring of the ham salting process. Methods for signal analysis: Time of flight calculation. *Journal of Food Engineering, 263*(October 2018), 87–95. https://doi.org/10.1016/j.jfoodeng.2019.05.032

Gibson, L. J., & Ashby, M. F. (1997). *Cellular Solids: Structure and Properties* (2nd Edition). Cambridge: Cambridge University Press.

Ginel, A. M., & Alvarez-Arenas, T. G. (2019). Air-coupled transducers for quality control in the food industry. In *IEEE international ultrasonics symposium* (pp. 803–806). IUS. https://doi.org/10.1109/ULTSYM.2019.8925853, 2019-Octob.

Golmohammadi, A., & Afkari-Sayyah, A. H. (2013). Long-term storage effects on the physical properties of the potato. *International Journal of Food Properties, 16*(1), 104–113. https://doi.org/10.1080/10942912.2010.529978

Ha, K. L., Kanai, H., Chubachi, N., & Kamimura, K. (1991). A basic study on nondestructive evaluation of potatoes using ultrasound. *Japanese Journal of Applied Physics, 30*, 80–82. https://doi.org/10.7567/JJAPS.30S1.80

Halil, T., Tamer, C. E., Suna, S., & Özkan Karabacak, A. (2020). Investigations of some quality parameters and mathematical modeling of dried functional chips. *Heat and Mass Transfer/Waerme- Und Stoffuebertragung, 56*(4), 1099–1115. https://doi.org/10.1007/s00231-019-02757-0

Hassini, L., Azzouz, S., Peczalski, R., & Belghith, A. (2007). Estimation of potato moisture diffusivity from convective drying kinetics with correction for shrinkage. *Journal of Food Engineering, 79*(1), 47–56. https://doi.org/10.1016/j.jfoodeng.2006.01.025

Jabeen, R., Aijaz, T., & Gul, K. (2015). Drying kinetics of potato using a self-designed cabinet dryer. *Cogent Food & Agriculture, 1*(1), Article 1036485. https://doi.org/10.1080/23311932.2015.1036485

Jambrak, A. R., Nutrizio, M., Djekić, I., Pleslić, S., & Chemat, F. (2021). Internet of nonthermal food processing technologies (Iontp): Food industry 4.0 and sustainability. *Applied Sciences, 11*(2), 1–20. https://doi.org/10.3390/app11020686

Kelly, S. P., Hayward, G., & Gomez, T. E. (2001). *AN air-coupled ultrasonic matching layer employing half wavelength cavity resonance*. Ultrasonics.

Kerhervé, S. O., Guillermic, R. M., Strybulevych, A., Hatcher, D. W., Scanlon, M. G., & Page, J. H. (2019). Online non-contact quality control of noodle dough using ultrasound. *Food Control, 104*(April), 349–357. https://doi.org/10.1016/j.foodcont.2019.04.024

Kim, K. B., Lee, S., Kim, M. S., & Cho, B. K. (2009). Determination of apple firmness by nondestructive ultrasonic measurement. *Postharvest Biology and Technology, 52*(1), 44–48. https://doi.org/10.1016/j.postharvbio.2008.04.006

Kingcam, R., Devahastin, S., & Chiewchan, N. (2008). Effect of starch retrogradation on texture of potato chips produced by low-pressure superheated steam drying. *Journal of Food Engineering, 89*(1), 72–79. https://doi.org/10.1016/j.jfoodeng.2008.04.008

Koksel, F., Scanlon, M. G., & Page, J. H. (2016). Ultrasound as a tool to study bubbles in dough and dough mechanical properties: A review. *Food Research International, 89*, 74–89. https://doi.org/10.1016/j.foodres.2016.09.015

Krokida, M. K., Karathanos, V. T., & Maroulis, Z. B. (2000). *Drying Technology : An International Journal COMPRESSION ANALYSIS OF DEHYDRATED AGRICULTURAL PRODUCTS*, 37–41. April 2013.

Laugier, P., & Haiat, G. (2016). Bone quantitative ultrasound. In *Clinical calcium* (Vol. 26). Issue 1.

Li, R., Lin, D., Roos, Y. H., & Miao, S. (2019). Glass transition, structural relaxation and stability of spray-dried amorphous food solids: A review. *Drying Technology, 37*(3), 287–300. https://doi.org/10.1080/07373937.2018.1459680

McClements, D. J. (1997). Ultrasonic characterization of foods and drinks: Principles, methods, and applications. *Critical Reviews in Food Science and Nutrition, 37*(1), 1–46. https://doi.org/10.1080/10408399709527766

Mizrach, A. (2008). Ultrasonic technology for quality evaluation of fresh fruit and vegetables in pre- and postharvest processes. *Postharvest Biology and Technology, 48*(3), 315–330. https://doi.org/10.1016/j.postharvbio.2007.10.018

Mohd Khairi, M. T., Ibrahim, S., Md Yunus, M. A., & Faramarzi, M. (2016). Contact and non-contact ultrasonic measurement in the food industry: A review. *Measurement Science and Technology, 27*(1). https://doi.org/10.1088/0957-0233/27/1/012001

Nguyen, T. K., Mondor, M., & Ratti, C. (2018). Shrinkage of cellular food during air drying. *Journal of Food Engineering, 230*, 8–17. https://doi.org/10.1016/j.jfoodeng.2018.02.017

Nielsen, S. S. (2010). *Food analysis* (IV ed.). Springer. https://doi.org/10.1007/978-1-4419-1478-1_6

Nielsen, M., & Martens, H. J. (1997). Low frequency ultrasonics for texture measurements in cooked carrots (Daucus carota L.). *Journal of Food Science, 62*(6), 1167–1171. https://doi.org/10.1111/j.1365-2621.1997.tb12237.x

Ozuna, C., Álvarez-Arenas, T. G., Riera, E., Cárcel, J. A., & Garcia-Perez, J. V. (2014). Influence of material structure on air-borne ultrasonic application in drying. *Ultrasonics Sonochemistry, 21*(3), 1235–1243. https://doi.org/10.1016/j.ultsonch.2013.12.015

Salazar, J., Chávez, J., Turó, A., & García-Hernández, M. J. (2017). Ultrasound in food processing recent advances. In *Ultrasound in food processing recent advances*.

Silva, K. S., Polachini, T. C., Luna-Flores, M., Luna-Solano, G., Resende, O., & Telis-Romero, J. (2021). Sorption isotherms and thermodynamic properties of wheat malt under storage conditions. *Journal of Food Process Engineering, 44*(9), 1–12. https://doi.org/10.1111/jfpe.13784

Sinha, A., & Bhargav, A. (2020a). Effect of state transition, drying kinetics and moisture content on Young's modulus variation during thermal drying of hygroscopic food materials. *Journal of Food Engineering, 279*(December 2019), Article 109957. https://doi.org/10.1016/j.jfoodeng.2020.109957

Sinha, A., & Bhargav, A. (2020b). Young's modulus estimation in food samples: Effect of experimental parameters. *Mechanics & Industry, 21*(4), 404. https://doi.org/10.1051/meca/2020025

Soltani Firouz, M., Farahmandi, A., & Hosseinpour, S. (2019). Recent advances in ultrasound application as a novel technique in analysis, processing and quality control of fruits, juices and dairy products industries: A review. *Ultrasonics Sonochemistry, 57*(May), 73–88. https://doi.org/10.1016/j.ultsonch.2019.05.014

Tian, S., & Xu, H. (2022). Nondestructive methods for the quality assessment of fruits and vegetables considering their physical and biological variability. *Food Engineering Reviews*. , Article 0123456789. https://doi.org/10.1007/s12393-021-09300-0

Xiaobo, Z., Xiaowei, H., & Povey, M. (2016). Non-invasive sensing for food reassurance. *The Analyst, 141*(5), 1587–1610. https://doi.org/10.1039/c5an02152a